

FACILE PREPARATION OF α -Fe₂O₃ NANOBULK VIA BUBBLE ELECTROSPINNING AND THERMAL TREATMENT

by

**Peng LIU^a, Chun-Hui HE^b, Fujuan LIU^a, Lan XU^a,
Yuqin WAN^c, and Ji-Huan HE^{a,*}**

^a National Engineering Laboratory for Modern Silk, College of Textile and Clothing Engineering, Soochow University, Suzhou, China

^b Nantong Bubbfil Nanotechnology Company Limited, Nantong, China

^c College of Textiles and Clothing, Jiangnan University, Wuxi, China

Original scientific paper
DOI: 10.2298/TSCI1603967L

In this work, α -Fe₂O₃ nanobulk with high aspect ratio were successfully prepared via a facile bubble electrospinning technique using polyvinylidene fluoride and iron chloride hexahydrate (FeCl₃·6H₂O) as α -Fe₂O₃ precursor followed by annealing in air at 600 °C. The products were characterized with field emission scanning electron microscope, Fourier transform infrared, X-ray photoelectron spectroscopy, and thermogravimetric analysis. The results showed that α -Fe₂O₃ nanobulk has a hierarchical heterostructure which has an extremely broad application prospect in many areas.

Key word: α -Fe₂O₃, bubble electrospinning, composite nanofibers, polyvinylidene fluoride

Introduction

In recent decades, transition metal oxide nanostructures have attracted considerable attention due to their widely applications. In particular, hematite (α -Fe₂O₃) is found to be promising in a variety of applications because of its high thermal stability under ambient conditions, environmentally friendly features and low production cost. Many α -Fe₂O₃ nanostructures, such as hollow fibers [1], nanotubes [2], and nanoporous [3], nanorods [4], and their various applications, such as gas sensors [5], catalysts [6], electrode materials [7], and adsorption materials [8] have been reported.

Compared to other means, such as chemical vapor deposition [9] and hydrothermal growth [10], bubble electrospinning [11-16] is the most effective and versatile approach for fabrication of functional nanomaterials, which using high voltage to produce ultrathin fibers with diameters ranging from a few to several hundred nanometers. For example, Liu *et al.* [17] have obtained electrospun membrane with superhydrophobic-supperpleophilic performance. Liu *et al.* [18] developed a novel manufacturing approach which is based on bubble electrospinning technology to fabricate nanofiber yarns. Liu *et al.* [19] have presented a novel technique which

* Corresponding author; e-mail: hejihuan@suda.edu.cn

called needle-disk electrospinning to enhance nanofibers throughput and fabricate nanofibers from various materials with high quality.

In this research, PVDF/ FeCl₃·6H₂O composite nanofibers were prepared using solution mixtures of iron(III) chloride hexahydrate (FeCl₃·6H₂O) and polyvinylidene fluoride (PVDF) via bubble electrospinning. Subsequently, the as-spun composite nanofibers were annealed in air at high temperature with an appropriate heating rate to form α -Fe₂O₃ nanobulk. The morphology, chemical, and thermal properties of the resultant α -Fe₂O₃ nanobulk were investigated through different approaches.

Experiment

In this work, 2.4g PVDF powder was added into acetone and dimethylformamide (DMF) mixed solvent (weight ratio = 1 : 1) and magnetically stirred for about 3 hours for 8 wt.% PVDF solution. Then different amount of FeCl₃·6H₂O was added into the previously prepared PVDF solution with magnetic stirring for 6 hours at room temperature to form a homogeneous solution. The concentration of FeCl₃·6H₂O (*i. e.*, 2, 6, and 10 wt.%) in the mixture was calculated based on the weight of PVDF.

The bubble electrospinning set-up used in this study can be found in our previous report [11, 12]. In a typical process, the solution was loaded into a U-shape groove with a stainless steel circular ring with an inner diameter of 1 cm. The circular ring which was charged by a high direct current voltage power supply was used as the positive electrode. A voltage of 25 kV was applied to the solution via the stainless steel circular ring. A piece of aluminum frame was grounded and used as nanofiber collector. The collecting distance between the circular ring and aluminum foil collector was 16 cm. All spinning processes were conducted at ambient temperature with a relatively low humidity.

The as-spun PVDF/FeCl₃·6H₂O composite nanofibers obtained with 2 wt.% FeCl₃·6H₂O were calcined in air at 600 °C for 3 hours with a rising rate of 10 °C per min to remove all organic residuals. After cooling to the room temperature, dark red α -Fe₂O₃ nanobulk were yield.

Results and discussion

The field emission scanning electron microscopy (FESEM) images and diameter distribution curves of as-spun FeCl₃·6H₂O/PVDF composite nanofibers with different contents (0, 2, 6, and 10 wt.%) are shown in fig. 1. It can be seen that pure PVDF nanofibers have a beaded morphology as show in fig. 1(a). Figure 1(b) shows that the as-spun pure PVDF nanofibers are basically smooth and relatively uniform apart from the beads.

In contrast with pure PVDF nanofibers, the composite nanofibers with different contents of FeCl₃·6H₂O are all beads free, as shown in fig. 1(c, e, g). This is due to the enhanced solution conductivity contributed by the presence of iron(III) ion. However, it is clearly observed in the fig. 1(d, f, h) that as the FeCl₃·6H₂O content increases, the surface roughness of FeCl₃·6H₂O/PVDF composite nanofibers increases. Figure 1(g) displays an interesting structure with interconnected branch-like junction.

Figure 1(A)-(D) shows the diameter distribution curves of as-spun nanofibers. The average diameters of pure PVDF nanofibers and composite nanofibers with different content of FeCl₃·6H₂O (2, 6, and 10 wt.%) are around 119.8, 23.9, 64.3, 11.8, 152.1, 27.1, and 215.9, 39.3 nm, respectively. With 2 wt.% addition of FeCl₃·6H₂O, the fibers diameter decreases. Smaller fiber diameter is desirable as it provides higher surface to volume ratio. However, the average diameter of the composite nanofibers dramatically increased as the concentration of

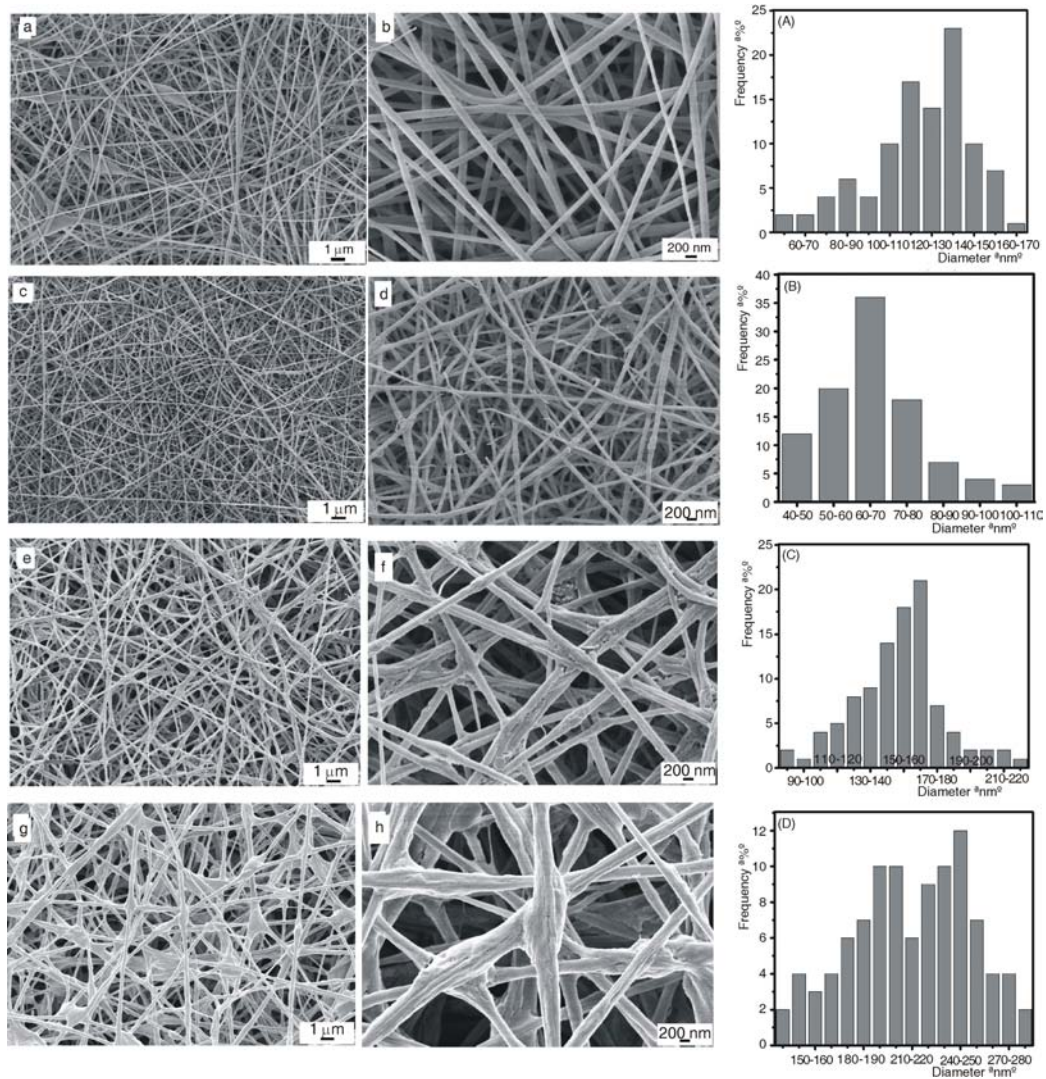


Figure 1. The FESEM images and diameter distribution of FeCl₃·6H₂O/PVDF composite nanofibers with different FeCl₃·6H₂O contents: (a, b, A) 0 wt.%, (c, d, B) 2 wt.%, (e, f, C) 6 wt.%, and (g, h, D) 10 wt.%

FeCl₃·6H₂O increased to 6 wt.% and 10 wt.%. This may be due to the increased solution viscosity caused by the high proportion of FeCl₃·6H₂O which weakened the spinnability of the solution. Among all the composite nanofibers, the composite nanofibers with 2 wt.% FeCl₃·6H₂O exhibited the smallest average diameter and narrowest scope of diameter distribution.

Figure 2 shows FESEM images of the α -Fe₂O₃ nanobulk with 2 wt.% FeCl₃·6H₂O obtained after thermal treatment in ambient air at 600 °C for 3 hours. It is clearly observed that the nanobulk is composed of large amounts of nanoparticles about 30 nm and nanoflakes with different high aspect ratios.

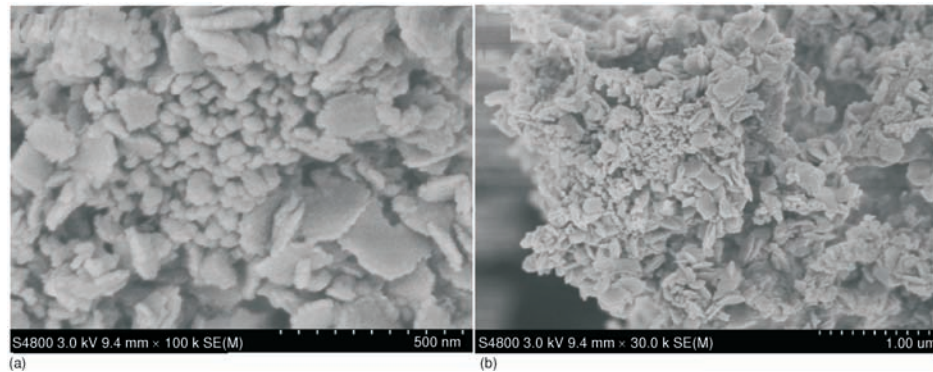


Figure 2. The FESEM images of as-calcined α -Fe₂O₃ nanobulk with 2 wt.% FeCl₃·6H₂O

The X-ray photoelectron spectroscopy (XPS) spectra was carried out to investigate the elemental composition and surface valence states of the α -Fe₂O₃ nanobulk, and the results are showed in fig. 3. The survey XPS curves in fig. 3(a) reveal that the sample is composed of Fe and O elements. Figure 3(b) exhibits the spectrum of Fe 2p region, in which the double individual peaks at

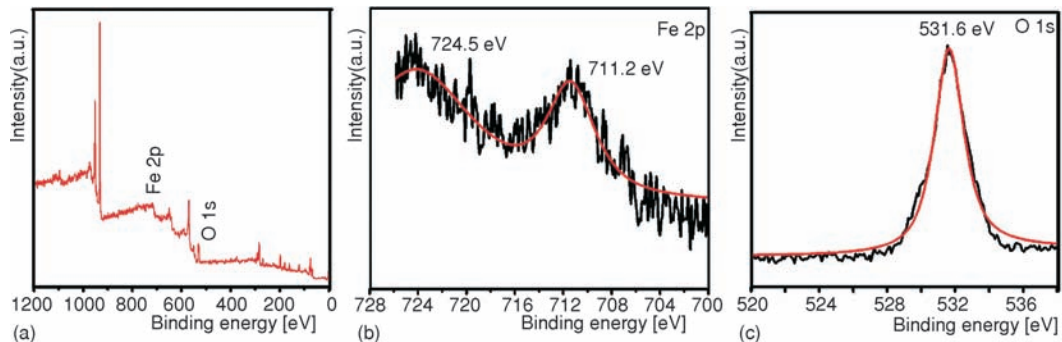


Figure 3. The XPS spectra of α -Fe₂O₃ (a) survey spectrum; (b) Fe 2p spectrum; (c) O 1s spectrum

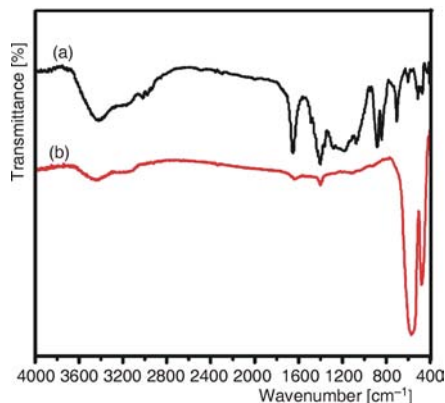


Figure 4. The FTIR spectra of FeCl₃·6H₂O/PVDF composite fibers (a) and α -Fe₂O₃ nanobulk (b)

711.2 and 724.5 eV correspond to Fe 2p_{3/2} and Fe 2p_{1/2}, respectively [1]. As shown in fig. 3(c), the characteristic peak of O1s with strong photoelectron signal at 531.6 eV, can be assigned to the Fe-O-Fe bonds. This result further proves α -Fe₂O₃ nanobulk was successfully synthesized.

To further verify the formation of α -Fe₂O₃ structure, Fourier transform infrared (FTIR) analysis was employed. Figure 4 shows the FTIR spectra of FeCl₃·6H₂O/PVDF composite fibers and α -Fe₂O₃ nanobulk calcined at 600 °C. A broad peak at about 3440 cm⁻¹ corresponds to H-OH stretch is clearly observed in fig. 4(a) [8].

The characteristic peaks of CH symmetric and CH₂ asymmetric vibration, CF₂ deforma-

tion and stretching vibrations corresponding to PVDF appeared at 2940 and 2850, 1400, 1180, and 883 cm⁻¹, respectively [20]. Those characteristic peaks disappeared and some new characteristic peaks appeared in α -Fe₂O₃ nanobulk as shown in fig. 4(b). The two sharp peaks appearing at 478 and 573 cm⁻¹ are assigned to the Fe-O vibration of the α -Fe₂O₃ nanobulk [7].

In order to elucidate the α -Fe₂O₃ nanobulk formation process, thermogravimetric analysis (TGA) analysis was carried out on the as-spun FeCl₃·6H₂O/PVDF precursor composite nanofibers. Figure 5 shows TGA curves of the as-spun FeCl₃·6H₂O/PVDF precursor composite nanofibers in the temperature range of 50-600 °C. It is clear that the first weight loss of 12.8% occurred at around 50-250 °C resulting from the

evaporation of absorbed water, residual DMF, acetone and the removal of crystal water molecules of the chlorides, which is an endothermic reaction. The second significant weight loss of approximately 31.7% from 250 °C to 360 °C can be ascribed to the partially decomposition of iron chloride and the degradation of the side chain of PVDF. These processes are accompanied by exothermic reaction. The third weight loss of 12.7% happened in the range of 360-600 °C, which could be attributed to the oxidative decomposition of the main chains of PVDF and the complete decomposition of iron chloride.

Finally, the total weight loss amounts to 57.2%, led to significant volume decrease and the formation of α -Fe₂O₃ nanobulk.

Conclusions

The PVDF/FeCl₃·6H₂O composite nanofibers with different content of FeCl₃·6H₂O (0, 2, 6, and 10 wt.%) were successfully manufactured by bubble electrospinning technique using PVDF and FeCl₃·6H₂O. The composite fibers of PVDF/FeCl₃·6H₂O with 2 wt.% FeCl₃·6H₂O was calcined at 600 °C to form the α -Fe₂O₃ nanobulk.

The SEM images indicates composite nanofibers with 2 wt.% FeCl₃·6H₂O exhibited smallest average diameter and the narrowest scope of diameter distribution. The formation of α -Fe₂O₃ was confirmed by FTIR, XPS, and TGA analysis. This α -Fe₂O₃ nanobulk can be widely used for many applications, such as gas sensors, catalysts, electrode materials, and absorption materials. This technique is applicable to preparation of other multifunctional nanomaterials as well.

Acknowledgment

The work is supported by Priority Academic Program Development of Jiangsu Higher Education Institutions (PAPD), National Natural Science Foundation of China under grant No. 51203066, No. 61303236, No. 11372205, and No. 51403143 and Project for Six Kinds of Top Talents in Jiangsu Province under grant No. ZBZZ-035, Science & Technology Pillar Program of Jiangsu Province under grant No. BE2013072, Natural Science Foundation of Jiangsu Province under Grant No. BK20140398, Natural Science Foundation of the Jiangsu Higher Education Institutions of China (Grant No. 14KJA130001), Production and Research Prospective

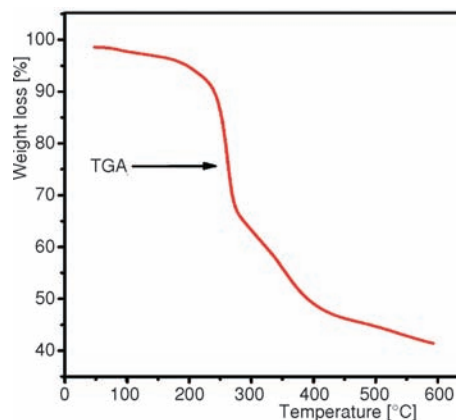


Figure 5. The TGA curves of FeCl₃·6H₂O/PVDF composite nanofibers

Joint Research Project of Jiangsu Province under grant No. 2015047-09. Research and Innovation Project for College Graduates of Jiangsu Province under grant NO. SJZZ15_0162.

References

- [1] Cheng, Y. L., et al., Formation Mechanism of Fe₂O₃ Hollow Fibers by Direct Annealing of the Electrospun Composite Fibers and Their Magnetic, Electrochemical Properties, *Cryst. Eng. Comm.*, 13 (2011), 8, pp. 2863-2870
- [2] Shao, H., et al., Preparation of α -Fe₂O₃ Nanotubes via Electrospinning and Research on Their Catalytic Properties, *Appl. Phys. A*, 108 (2012), 4, pp. 961-965
- [3] Sundaramurthy, J., et al., Superior Photocatalytic Behaviour of Novel 1D Nanobraid and Nanoporous α -Fe₂O₃ Structures, *RSCA Advances*, 2 (2012), 21, pp. 8201-8208
- [4] Christie, T. C., et al., Electrospun α -Fe₂O₃ Nanorods as a Stable, High Capacity Anode Material for Li-ion Batteries, *J. Mater. Chem.*, 22 (2012), 24, pp. 12198-12204
- [5] Yan, S., et al., A Novel Structure for Enhancing the Sensitivity of Gas Sensors- α -Fe₂O₃ Nanoropes Containing a Large Amount of Grain Boundaries and their Excellent Ethanol Sensing Performance, *J. Mater. Chem. A*, 3 (2015), 11, pp. 5982-5990
- [6] Dhal, J. P., et al., Synthesis, Characterization and Photocatalytic Application of Ultra-Fine α -Fe₂O₃ Nanofiber, *Asian Journal of Chemistry*, 25 (2013), June, pp. S22-S26
- [7] Chaudhari, S., et al., 1D Hollow α -Fe₂O₃ Electrospun Nanofibers as High Performance Anode Material for Lithium Ion Batteries, *J. Mater. Chem.*, 22 (2012), 43, pp. 23049-23056
- [8] Gao, Q., et al., Novel Hollow α -Fe₂O₃ Nanofibers via Electrospinning for Dye Adsorption, *Nanoscale Research Letters*, 10 (2015), Dec., pp. 176-183
- [9] Nazari, M., et al., Synthesis and Characterization of Maghemite Nanopowders by Chemical Precipitation Method, *J. Nanostruct. Chem.*, 4 (2014), June, pp. 99-103
- [10] Hua, J., et al., Hydrothermal Synthesis and Characterization of Monodisperse α -Fe₂O₃ Nanoparticles, *Materials Letters*, 63 (2009), 30, pp. 2725-2727
- [11] Chen, R. X., et al., Bubble Rupture in Bubble Electrospinning, *Thermal Science*, 19 (2015), 4, pp. 1141-1149
- [12] Dou, H., et al., A Belt-Like Superfine Film Fabrication by the Bubble-Electrospinning, *Thermal Science*, 17 (2013), 5, pp. 1508-1510
- [13] Shen, J., et al., Effect of Pore Size on Gas Resistance of Nanofiber Membrane by the Bubble Electrospinning, *Thermal Science*, 19 (2015), 4, pp. 1349-1351
- [14] He, J.-H., An Alternative Approach to Establishment of a Variational Principle for the Torsional Problem of Piezoelectric Beams, *Applied Mathematics Letters*, 52 (2016), Complete, pp. 1-3
- [15] Chen, R. X., et al., Series Solution of the Autocatalytic Hydrolysis of Cellulose, *Cellulose*, 18 (2015), 5, pp. 3099-3104
- [16] He, C. H., et al., Bubble Spinning for Fabrication of PVA Nanofibers, *Thermal Science*, 19 (2015), 2, pp. 743-746
- [17] Liu, Z., et al., Tunable Surface Morphology of Electrospun PMMA Fiber Using Binary Solvent, *Applied Surface Science*, 364 (2016), Feb., pp. 516-521
- [18] Liu, H. Y., et al., A Novel Method for Fabrication of Fascinated Nanofiber Yarns, *Thermal Science*, 19 (2015), 4, pp. 1331-1335
- [19] Liu, Z., et al., Active Generation of Multiple Jets for Production Nanofiber with High Quality and High Throughput, *Material & Design*, 94 (2016), Mar., pp. 496-501
- [20] Wang, Z. Y., et al., Preparation and Catalytic Property of PVDF Composite Membrane with Polymeric Spheres Decorated by Pd Nanoparticles in Membrane Pores, *Journal of Membrane Science*, 496 (2015), Dec., pp. 95-107

Paper submitted: December 16, 2015

Paper revised: February 10, 2016

Paper accepted: February 21, 2016